Enhanced properties of well-defined polymer networks prepared by a sequential thiol-Michael - radical thiol-ene strategy (STMRT)

Sergio Cespedes[a], Rachel A. Hand[b], Nikola Chmel[b], Graeme Moad[c], Daniel J. Keddie[d] and Tara L. Schiller[a]*

[a]WMG, University of Warwick, Coventry, CV4 7AL, UK

[b]Department of Chemistry, University of Warwick, Coventry, CV4 7AL, UK

[c]CSIRO Manufacturing, Bag 10, Clayton South, VIC 3169, Australia

[d]School of Sciences, Faculty of Science and Engineering, University of Wolverhampton, Wolverhampton, WV1 1LY, UK

ABSTRACT

A sequential thiol-Michael - radical thiol-ene (STMRT) strategy was used to produce poly(ethylene glycol)-based model networks and enable establishment of a structure-property relationship from the network characteristics. Selective double thiol-Michael reactions on a series of poly(ethylene glycol) diacrylates (PEGDA), that differed in average chain length, with two molar equivalents of the trithiol trimethylolpropane tris(3-mercaptopropionate) (TMPTMP) yielded well-defined telechelic poly(ethylene glycol)-based tetrathiols. These tetrathiols were in turn used to produce model (co-)networks by photo-induced radical thiol-ene polymerization with either the same poly(ethylene glycol) diacrylates or with tri(ethyleneglycol) divinylether (TEGDVE). The properties of these networks were studied by Fourier transform infrared spectroscopy (FTIR), differential scanning calorimetry (DSC) and dynamic mechanical thermal analysis (DMTA). The STMRT-produced model networks possess storage moduli (E') up to 4-fold larger and glass transition temperatures (T_g) of up to 10 °C lower than conventionally produced counterparts. The STMRT strategy allows the properties of the model networks to be finely tuned by manipulation of crosslink density and average polymer chain length.

KEYWORDS

Photopolymerization, thiol-Michael, network polymers, model networks, thiol-ene

INTRODUCTION

Radical-induced thiol-ene polymerization is a versatile and powerful reaction for the synthesis of polymer networks.[1, 2] Network formation via thiol-ene polymerization is a polyaddition reaction in which the reaction progresses by addition reactions between species of all chain lengths.[3] A consequence of this is that thiol-ene networks maintain relatively low viscosity throughout the polymerization until the gel point, which typically appears at much higher monomer conversions than for networks formed by chain polymerization (e.g. network formation from multifunctional (meth)acrylates).[4-7] Thus resulting in a more homogeneous distribution of crosslink points, less shrinkage, and reduced internal stress, as the chains can rearrange freely in a low viscosity medium throughout much of the reaction.[2] This results in improved adhesion of the thiol-ene network to all kinds of surfaces, which makes them ideal materials for use as adhesives and coatings.[8]

Thiol-ene polymerization proceeds through alternating steps of: (1) thiyl radical addition to an alkene resulting in a C-centred radical; and (2) hydrogen abstraction from a thiol by the C-centred radical to form a new thiyl radical. Neither of these two reaction steps show significant oxygen inhibition.[9] The rate of the reaction is often enhanced by the inclusion of a thermal or photoradical initiator.

Low shrinkage, rapid curing kinetics and tolerance of oxygen combine to make thiol-ene processes suitable for photocuring and lithography.[10-12] Despite the advantages described above, the thiol-ene reaction does have some limitations with respect to the substrate scope and the final materials properties. For example, the photo thiol-ene reaction can be very slow for substituted and/or conjugated olefins.[13, 14] Therefore, the reaction is typically restricted to the use of alkenes with terminal, vinyl groups (e.g. R-CH=CH_2). Due to the polyaddition nature of the thiol-ene reaction, thiol-ene networks generally have a low crosslink density. This directly influences the physical properties of the resulting materials; they are usually soft, flexible materials, displaying low but well-defined glass transition temperatures (T_g,) high storage moduli (E'), and high thermal stability.[15]

Many approaches for controlling the mechanical properties of thiol-ene-based networks have been explored.[16-18] For example, introducing some thiols into polyacrylate-based resins combines both polyaddition and chain homopolymerization.[9] However, it is not possible to control network architecture or to introduce enough thiol to significantly alter the T_g. However, more highly functionalized thiols and/or enes have been reported. For example, Wood *et al.* used hexathiols,[19] while Rehnberg *et al.*[20] compared the effect of level of functionality by comparing a monomer bearing 16 terminal allyl ether groups with a triallyl compound. Bowman *et al.* have proposed thiol-yne chemistry as an alternative to thiol-ene to increase functionality (each alkyne can add two thiol groups).[20] Base-catalysed photo networks were introduced by the Bowman group in a step-wise procedure without further refinement prior to making networks.[21] These approaches have shown some success; however, they demonstrate a decrease in conversion with an increase in functionality.

Herein, we present a modular method to produce poly(ethylene glycol)-based model networks of defined structure using a combination of base-catalysed thiol-Michael addition and radical thiol-ene (i.e. sequential thiol-Michael radical thiol-ene, STMRT). The resultant networks were analysed by photo infrared spectroscopy (FTIR) isothermal photo differential scanning calorimetry (DSC) and dynamic mechanical thermal analysis (DMTA) to provide insight into the effect of tetrathiol

macromonomer chain length on the materials properties. Direct comparison between STMRT-prepared materials and analogous polymers prepared via a traditional thiol-ene polymerization route reveals that the STMRT strategy delivers materials with both significantly higher storage moduli (E') and lower T_g.

EXPERIMENTAL

Materials.

Poly(ethylene glycol) diacrylate of M_n= 250 g/mol ($X_n \approx 3$, PEG_3DA, **1**), M_n = 575 g/mol ($X_n \approx 10$, $PEG_{10}DA$, **2**), and M_n = 700 g/mol ($X_n \approx 13$, $PEG_{13}DA$, **3**), tri(ethylene glycol) divinyl ether (TEGDVE), trimethylolpropane tris(3-mercaptopropionate) (TMPTMP), benzoin ethyl ether (BEE), methanol and deuterated chloroform ($CDCl_3$) were purchased from Sigma-Aldrich and used without further purification.

Characterization.

Nuclear magnetic resonance (NMR) spectra were recorded on a Joel 400 MHz JNM-ECZ400R/M1 spectrometer at room temperature in deuterated chloroform ($CDCl_3$). ^1H and ^{13}C NMR spectra were internally referenced to residual solvent.[22] Gel permeation chromatography (GPC) was performed on an Agilent Infinity II MDS instrument equipped with differential refractive index (DRI), viscometry (VS), dual angle light scatter (LS) and variable wavelength UV detectors. The system was equipped with 2 x PLgel Mixed D columns (300 x 7.5 mm) and a PLgel 5 µm guard column. The eluent was *N*,*N*-dimethylformamide (DMF) (containing 5 mmol/L ammonium tetrafluoroborate (NH_4BF_4) additive). Samples were run at 1 mL/min at 50 °C. Number (M_n) and weight-average (M_w) molar mass and molar mass dispersity ($Đ$) data was evaluated using Agilent GPC/SEC software. The GPC columns were calibrated with low dispersity poly(methyl methacrylate) (PMMA) standards (Agilent EasyVials) ranging from 550 to 955,000 g·mol^{-1} and molar masses are reported in PMMA equivalents. A 3rd order polynomial was used to fit the log M_p vs. time calibration curve, which was linear across the molar mass ranges. All GPC samples were filtered through a nylon membrane with 0.22 µm pore size before injection.

Dynamic mechanical thermal analysis (DMTA) was performed with a PerkinElmer DMA8000 with single cantilever geometry on specimens of approximately 1 mm × 6 mm × 40 mm using a strain of 0.02 %, at a frequency of 1 Hz and a heating rate of 2 °C min^{-1} over a temperature range of −80 to 20 °C. The temperature when tan δ reaches maximum value (inflection point of E') is recorded as the T_g of the polymer.

Poly(ethylene glycol)-based tetrathiol macromonomer synthesis.

The synthetic method provided for the PEG_3-tetrathiol macromonomer **(4)** is typical. The diacrylate used, the yield and characterization data are listed below for the other PEG-tetrathiols **5** and **6**.

Synthesis PEG_3-tetrathiol macromonomer (4):

To a stirred mixture of PEG_3DA **1** (1.250 g, 5.0 mmol, 1 equiv.) and TMPTMP (4.0 g, 10.0 mmol, 2 equiv.) was added *n*-hexylamine (13.0 µL, 0.1 mmol, 0.02 equiv., 1 mol%). The reaction was stirred for a further 2 h to allow the reaction to proceed to completion. The resultant crude product was triturated with methanol (2 × 5 mL). Following removal of solvent under reduced pressure the PEG_3-tetrathiol macromonomer **4** was isolated as a viscous liquid (3.78 g, 3.6 mmol, 72 %); ^1H NMR (400

MHz, $CDCl_3$): δ 0.88 (m, 6H, 2 × CH_2CH_3), 1.47 (m, 4H, 2 × CH_2CH_3), 1.61 (m, 4H, 4 × SH), 2.65 (m, 16H, 8 × CO-CH_2-CH_2-S), 2.76 (m, 16H, 8 × O=C-CH_2-CH_2-S), 3.64 (br s, ~4H, ~1 × O-CH_2-CH_2-O), 3.69 (m, 4H, 2 × O=CO-CH_2-CH_2O), 4.05 (m, 12H, 6 × CH_2C*), 4.24 (m, 4H, 2 × O=COCH_2CH_2O); ^{13}C NMR (50 MHz, $CDCl_3$): δ 7.3 (2 × CH_3), 19.7 (4 × CH_2SH), 22.9 (2 × CH_2CH_3), 26.9 (2 × CH_2SCH_2), 26.9 (2 × CH_2SCH_2), 34.5 (2 × $CH_2SCH_2CH_2$C=O), 34.6 (2 × $CH_2SCH_2CH_2$C=O), 38.3 (2 × $HSCH_2CH_2$C=O), 40.7 (2 × H_3CH_2CC*), 63.8 (6 × O=COCH_2C* & 2 × O=COCH_2CH_2), 69.1 (2 × O=COCH_2CH_2O), 70.5 (~1 × OCH_2CH_2O), 171.4 (4 × C=O), 171.5 (2 × C=O), 171.9 (2 × C=O).

Synthesis PEG_{10}-tetrathiol macromonomer (5):

The reaction of TMPTMP and PEG_{10}DA (2.87 g, 5.0 mmol, 1 equiv.) using the above procedure gave the PEG_{10}-tetrathiol macromonomer **5** (5.6 g, 4.1 mmol, 83 %); ^{1}H NMR (400 MHz, $CDCl_3$): δ 0.88 (m, 6H, 2 × CH_2CH_3), 1.47 (m, 4H, 2 × CH_2CH_3), 1.60 (m, 4H, 4 × SH), 2.63 (m, 16H, 8 × CO-CH_2-CH_2-S), 2.76 (m, 16H, 8 × O=C-CH_2-CH_2-S), 3.64 (br s, ~32H, ~8 × O-CH_2-CH_2-O), 3.68 (m, 4H, 2 × O=CO-CH_2-CH_2O), 4.04 (m, 12H, 6 × CH_2C*), 4.24 (m, 4H, 2 × O=COCH_2CH_2O); ^{13}C NMR (50 MHz, $CDCl_3$): δ 7.3 (2 × CH_3), 19.5 (4 × CH_2SH), 22.9 (2 × CH_2CH_3), 26.8 (2 × CH_2SCH_2), 26.9 (2 × CH_2SCH_2), 34.5 (2 × $CH_2SCH_2CH_2$C=O), 34.6 (2 × $CH_2SCH_2CH_2$C=O), 38.3 (2 × $HSCH_2CH_2$C=O), 40.7 (2 × H_3CH_2CC*), 63.8 (6 × O=COCH_2C* & 2 × O=COCH_2CH_2), 69.0 (2 × O=COCH_2CH_2O), 70.5 (~8 × OCH_2CH_2O), 171.2 (4 × C=O), 171.4 (2 × C=O), 171.7(2 × C=O).

Synthesis PEG_{13}-tetrathiol macromonomer (6):

The reaction of TMPTMP and PEG_{13}DA (3.50 g, 5.0 mmol, 1 equiv.) using the above procedure gave the PEG_{13}-tetrathiol macromonomer **6** (5.3 g, 3.55 mmol, 71 %); ^{1}H NMR (400 MHz, $CDCl_3$): δ 0.89 (m, 6H, 2 × CH_2CH_3), 1.48 (m, 4H, 2 × CH_2CH_3), 1.61 (m, 4H, 4 × SH), 2.63 (m, 16H, 8 × CO-CH_2-CH_2-S), 2.76 (m, 16H, 8 × O=C-CH_2-CH_2-S), 3.62 (br s, ~44H, ~11 × O-CH_2-CH_2-O), 3.68 (m, 4H, 2 × O=CO-CH_2-CH_2O), 4.05 (m, 12H, 6 × CH_2C*), 4.23 (m, 4H, 2 × O=COCH_2CH_2O); ^{13}C NMR (50 MHz, $CDCl_3$): δ 7.3 (2 × CH_3), 19.6 (4 × CH_2SH), 22.9 (2 × CH_2CH_3), 26.8 (2 × CH_2SCH_2), 26.9 (2 × CH_2SCH_2), 34.5 (2 × $CH_2SCH_2CH_2$C=O), 34.6 (2 × $CH_2SCH_2CH_2$C=O), 38.3 (2 × $HSCH_2CH_2$C=O), 40.7 (2 × H_3CH_2CC*), 63.8 (6 × O=COCH_2C* & 2 × O=COCH_2CH_2), 69.0 (2 × O=COCH_2CH_2O), 70.5 (~11 × OCH_2CH_2O), 171.2 (4 × C=O), 171.4 (2 × C=O), 171.7(2 × C=O).

Synthesis of poly(ethylene glycol)-based model networks by isothermal thiol-ene photopolymerization

Preparative synthesis of polymer networks for dynamic mechanical thermal analysis

Network polymers were prepared via photopolymerization. A typical mixture was prepared as follows: the reaction mixture approximately 1 g in total with 1% w/w of photoinitiator (BEE) (see Table 1 for sample identities, and Table S4 in the supporting information for the masses of reagents) was injected into 1 mm × 6 mm× 40 mm mould covered with a PET film to ensure thermal stability of sample. The sample was cured at a power of 8.2 mW·cm^{-2} with a 320 nm-390 nm filter and fibre optic light guide attached to the light source (Omnicure S2000) for a total of 20 min. UV intensity was measured with a radiometer, setting the slit at 50% and a distance of 10 cm to the sample. The samples were stored in the dark for approximately 24 h at room temperature prior to analysis, to ensure reproducibility of the results.[23]

Curing analysis via photo-differential scanning calorimetry

Enthalpies of reaction for photopolymerization *via in-situ* photo-differential scanning calorimetry (photo-DSC)[24] of duplicate reaction mixtures during cure were measured and analysed; photopolymerization of the monomers was performed on samples of ~5 mg in open aluminium pans in a N_2 flow at 20 °C with a Perkin Elmer DSC-6000 (Perkin Elmer, UK) equipped with an Intracooler. The irradiation intensity of the light source at the sample pans was 8.2 mW cm^{-2} with a 320-390 nm filter in place, by setting the slit to 5% and distance to 2cm. Allowance for the thermal imbalance due to the irradiation was made by repeating the irradiation of the cured sample in a second isothermal photoDSC run and subtracting the data from the first run.[25, 26] No further polymerization was observed for any sample during the repeated irradiation. Enthalpy of reaction was obtained by integration of the exotherm peak.

Curing analysis via photo-Fourier transform infrared spectroscopy

Consumption of the thiol and alkene functional groups of duplicate reaction mixtures during cure was measured by photo-FTIR using a Jasco 4200, equipped with ZnGeSe mirror and Mercury Cadmium Telluride (MCT-M) detector cooled by liquid nitrogen. The chamber and optics were constantly purged with a flow of nitrogen and the angle of incidence was set to 70°C. The instrument was ready for analysis when no CO_2 peak could be observed. The chamber was kept open but covered with a handcrafted lid to protect it from light. Absorbance spectra were captured in single accumulation at a rate of one scan every 2 s. The final conversion was determined by averaging the values obtained after reaction has gone to completion, which correlates to the average of 15 data points. The mirror was cleaned with acetone between samples and air dried. The light source for the experiment was a mercury arc lamp (Omnicure S2000) equipped with a 365 nm filter and a light guide that pierces the FTIR lid. The distance from the light guide to the mirror was 2 cm, and the slit was open to 5% to obtain a radiance intensity of 8.2 mW/cm^2 centred over the mirror.

The heat of reaction can be estimated from photo-FTIR conversion data of thiol-vinyl ether-acrylate systems. Assuming that vinyl ether homopolymerisation does not take place, and neglecting acrylate to vinyl ether cross-propagation, it follows that all vinyl ethers have reacted with thiols, the remaining thiols have reacted with acrylates, and the remaining acrylates have homopolymerized. This results in Equation 1:

Equation 1:

$$\Delta H \quad \Delta_{addVE}\,[VE]_0 \cdot \mu_{VE} + \Delta_{addACR}\,([SH]_0 \cdot \mu_{SH} - [VE]_0 \cdot \mu_{VE}) + \Delta H_{pol} \cdot \{[ACR]_0 \cdot \mu_{ACR} - ([SH]_0 \cdot \mu_{SH} - [VE]_0 \cdot \mu_{VE})\}$$

$$\Delta H_{per\ thiol} = \frac{\Delta H}{[SH]_0}$$

where $\Delta H_{per\ thiol}$ is the heat of reaction per mole of thiol in kJ/mol, ΔH is the heat of reaction in kJ/g, μ_i is conversion of the functional group *i* (as measured by FTIR), concentrations are expressed in mol/g, $\Delta H_{addVE} \approx$ -43.9 kJ/mol[27] is the standard heat of reaction for thiol-vinyl ether addition, ΔH_{addACR} is the standard heat of reaction for thiol-acrylate addition, -61.9 kJ/mol,[27] and ΔH_{pol} is the standard heat of reaction for acrylate homopolymerization, -86.2 kJ/mol.[28]

The enthalpy estimated from the photoFTIR conversion data is presented in Table 1 along with the enthalpy obtained empirically by photoDSC measurements for direct comparison. Full details of the photo-FTIR set up and sample preparation can be found in the Supporting Information.

Results and discussion

Synthesis of PEG-tetrathiol macromonomers (4-6)

PEG-based tetrathiols of differing chain lengths (**4**-**6**) were prepared via base-catalysed thiol-Michael reaction (see Scheme 1); the reaction of two molar equivalents of the trithiol TMPTMP with the relevant PEG diacrylate precursors (**1**-**3**) in the presence of *n*-hexylamine delivered the macromonomers in moderate to high yields (~70-80 %).

^{1}H and ^{13}C NMR analysis of the resulting materials indicates high purity, with no evidence of the aza-Michael products observed (see Figures S1-S6 in the supporting information). Furthermore, oligomerization appears to be minimal; comparison of the integrals for the thiol-adjacent carbons

Scheme 1: The synthesis of PEG-tetrathiol macromonomers (**4-6**) by *n*-hexylamine-catalysed selective double thiol-Michael addition of TMPTMP to PEG diacrylates (**1-3**)

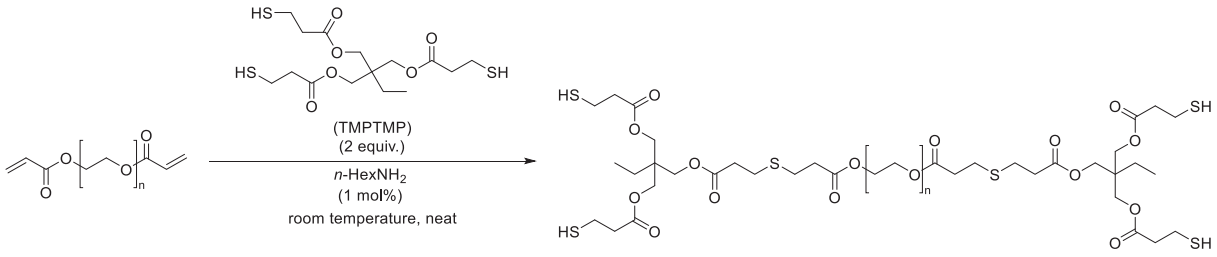

1 PEG_3DA, M_n=250
2 $PEG_{10}DA$, M_n=575
3 $PEG_{13}DA$, M_n=700

4 PEG_3-$(SH)_4$, 72% yield
5 PEG_{10}-$(SH)_4$, 83% yield
6 PEG_{13}-$(SH)_4$, 71% yield

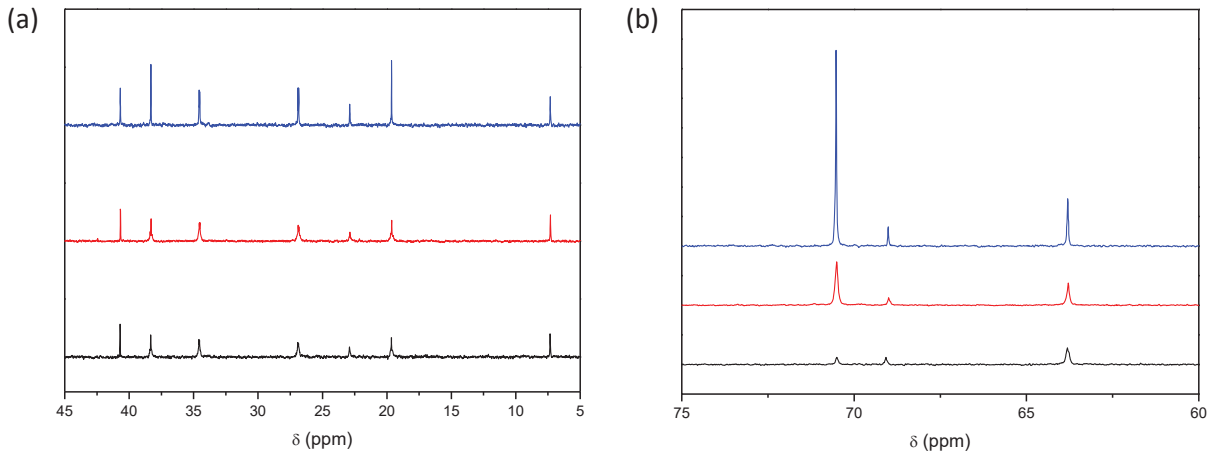

Figure 1: Expansions of the (a) aliphatic and (b) ether regions of the ^{13}C NMR spectra of **4** (black), **5** (red) and **6** (blue).

(i.e., 19.6 ppm) and sulphide-adjacent carbons (i.e. 26.8-26.9 ppm, see Figure 1 (a)) in the ^{13}C NMR gives ratios very close to the expected 4:4 for each of the tetrathiol macromonomers.[28,§] Additionally, the expected integral ratios are also observed for all the oxygen-adjacent carbon resonances (i.e. those between 60-75 ppm, see Figure 1(b))[§§] indicating no fractionation occurred during sample purification. Due to the low molar mass of the PEG-tetrathiols, GPC was of limited utility in their analysis.

Preparation of binary model networks through trithiol/diacrylate copolymerization

Prior to investigation of the materials prepared via the STMRT method, we sought to prepare benchmark systems for comparison using a standard thiol-ene polymerization methodology. To this end, we first investigated the photoinitiated radical copolymerization of the trithiol, TMPTMP, with a range of poly(ethylene glycol) diacrylates with various number average degrees of polymerization (**1**, X_n = ~3; **2**, X_n = ~10; **3**, X_n = ~13) (see samples **A-C** in Table 1).

In order to assess the extent of reaction between the thiol and acrylate groups in these systems, kinetic analyses were obtained from time-resolved photo-IR spectra. A representative example of photo-IR data analysed for the reaction between PEG_3DA **1** and TMPTMP (i.e. sample A, Table 1) is shown in the supporting information (for example see Figure S7 in the supporting information). The

Table 1: Details of network polymers prepared via thiol-ene photopolymerization

Sample[a]	diacrylate (DACR)	divinyl ether (DVE)	thiol (RSH)	[DA]:[DVE]:[RSH]	Network[b]	Photo-FTIR % conversion[c,g]			Photo-FTIR $\Delta H_{per\ thiol}$ (kJ/mol)[d,g]	DSC[e] $\Delta H_{reaction}$ (J/g)	DSC[e] $\Delta H_{per\ thiol}$ (kJ/mol)	DMA[f] T_g (°C)	DMA[f] *FWHM* (°C)	DMA[f] *E'* (MPa)
						SH	ACR	VE						
A	**1**	—	TMPTMP	3:0:2	*net*-poly(PEG_3DA-*co*-TMPTMP)	27%	94%	-	-74.5	-194.8	-50.8	-25.4	8.7	1.9
B	**2**	—	TMPTMP	3:0:2	*net*-poly(PEG_{10}DA-*co*-TMPTMP)	43%	92%	-	-68.9	-136.8	-57.8	-35.8	6.3	12.8
C	**3**	—	TMPTMP	3:0:2	*net*-poly(PEG_{13}DA-*co*-TMPTMP)	45%	98%	-	-73.5	-132.1	-64.5	-40.9	7.7	12.0
D	**1**	—	**4**	2:0:1	*net*-poly(PEG_3DA-*co*-TMPTMP)	39%	93%	-	-70.7	-127.8	-50	-28.2	10.9	6.7
E	**2**	—	**5**	2:0:1	*net*-poly(PEG_{10}DA-*co*-TMPTMP)	46%	89%	-	-65.5	-88.0	-55.9	-35.9	7.2	35.9
F	**3**	—	**6**	2:0:1	*net*-poly(PEG_{13}DA-*co*-TMPTMP)	44.6	94%	-	-70.1	-86.8	-63.6	-40.8	9.9	42.8
G	**1**	TEGDVE	TMPTMP	1:2:2	*net*-poly(PEG_3DA-*co*-TEGDVE-*co*-TMPTMP)	69%	94%	98%	-54.8	-121.5	-29.8	-25.5	7.8	5.1
H	**2**	TEGDVE	TMPTMP	1:2:2	*net*-poly(PEG_{10}DA-*co*-TEGDVE-*co*-TMPTMP)	93%	100%	90%	-46.9	-124.6	-37.2	-36.4	5.8	12.7
I	**3**	TEGDVE	TMPTMP	1:2:2	*net*-poly(PEG_{13}DA-*co*-TEGDVE-*co*-TMPTMP)	92%	99%	89%	-46.6	-145.3	-46.6	-37.9	5.6	13.6
J	—	TEGDVE	**4**	0:2:1	*net*-poly(PEG_3DA-*co*-TEGDVE-*co*-TMPTMP)	86%	-	98%	-45.9	-71.6	-26.3	-35.7	6.2	21.6
K	—	TEGDVE	**5**	0:2:1	*net*-poly(PEG_{10}DA-*co*-TEGDVE-*co*-TMPTMP)	59%	-	83%	-42.3	-65.2	-29.3	-41.1	6.1	13.8
L	—	TEGDVE	**6**	0:2:1	*net*-poly(PEG_{13}DA-*co*-TEGDVE-*co*-TMPTMP)	78%	-	82%	-37.0	-58.8	-28.3	-44.2	5.7	22.0

[a]All reactions initiated with 1% w/w BEE, [b]structure of the network in terms of commercially available monomer units, [c]Conversion quantified by peak height in photoFTIR, as described in supporting information, [d] Values obtained from Equation 1, [e]enthalpy values obtained from photo-DSC experiments, [f]values obtained from DMTA analysis, [g]the presented values only account for conversion of the thiols during the radical thiol-ene photopolymerisation. The conversion of thiols during the thiol-Michael addition of STMRT is ignored in this table for both conversion and *ΔH*

consumption of C_{sp2} vinyl groups can clearly be seen by the disappearance of the C_{sp2}=C_{sp2} double bond stretching frequency at 1660-1600 cm^{-1} and increase in the C_{sp3}-H stretching band(for example see Figure S8 in the Supporting Information).[29] The reduction of the band C_{sp2}=C_{sp2} out-of-plane stretch, at 820-800 cm^{-1} and the shift in the C=O stretching band at 1730 cm^{-1} to higher wavenumber is indicative of loss of conjugation and therefore consistent with acrylate consumption.[30] The S-H peak is weak at 2560 cm^{-1}. A decrease in intensity is observed, although the rate of conversion is lower than that seen for the acrylate functional groups (see Figure 2 (a), A-C).[29] This is indicative of a faster consumption of acrylate than of thiols; concurrent acrylate homopolymerization occurs as expected.[31, 32] The exact method for the quantification of peak height in FTIR is detailed in supporting information, and in figures S9 to S14 also in supporting information.

The peak heights of the thiol peak at ≈2560 cm^{-1} and alkene at ≈1636 cm^{-1} were used to estimate conversion of the functional groups under conditions that mimic those of the moulding (sample used for DMA analysis), as described in Materials and Methods. The conversion of thiol and acrylate

over time is shown in Figure 2 (a) for the samples **A-C**. The final conversion of acrylate groups is estimated as 94%, 92%, and 98% for samples **A, B** and **C** respectively (see Table 1). Thiol conversion is estimated as 27%, 43%, and 45% for samples **A, B** and **C** respectively (see Table 1). Theoretical heat of reaction per thiol, calculated using the photo-FTIR conversion data, corresponded well with that obtained experimentally via photo-DSC (see Table 1 and Figure S16 in the supporting information).

The difference between the conversion of acrylate and thiol groups is caused by the concurrent consumption of acrylate groups *via* conventional radical polymerization.[31, 32] Interestingly, an increase in PEG chain length appears to promote thiol-ene reaction as evidenced by thiol conversion (see Table 1, samples A-C and Figure 2).

The materials properties of the networks **A-C** were analysed using DMA (see Table 1 and Figure 2(c), solid lines). These materials display the expected trends in T_g; the T_g was found to decrease with increasing PEG length.

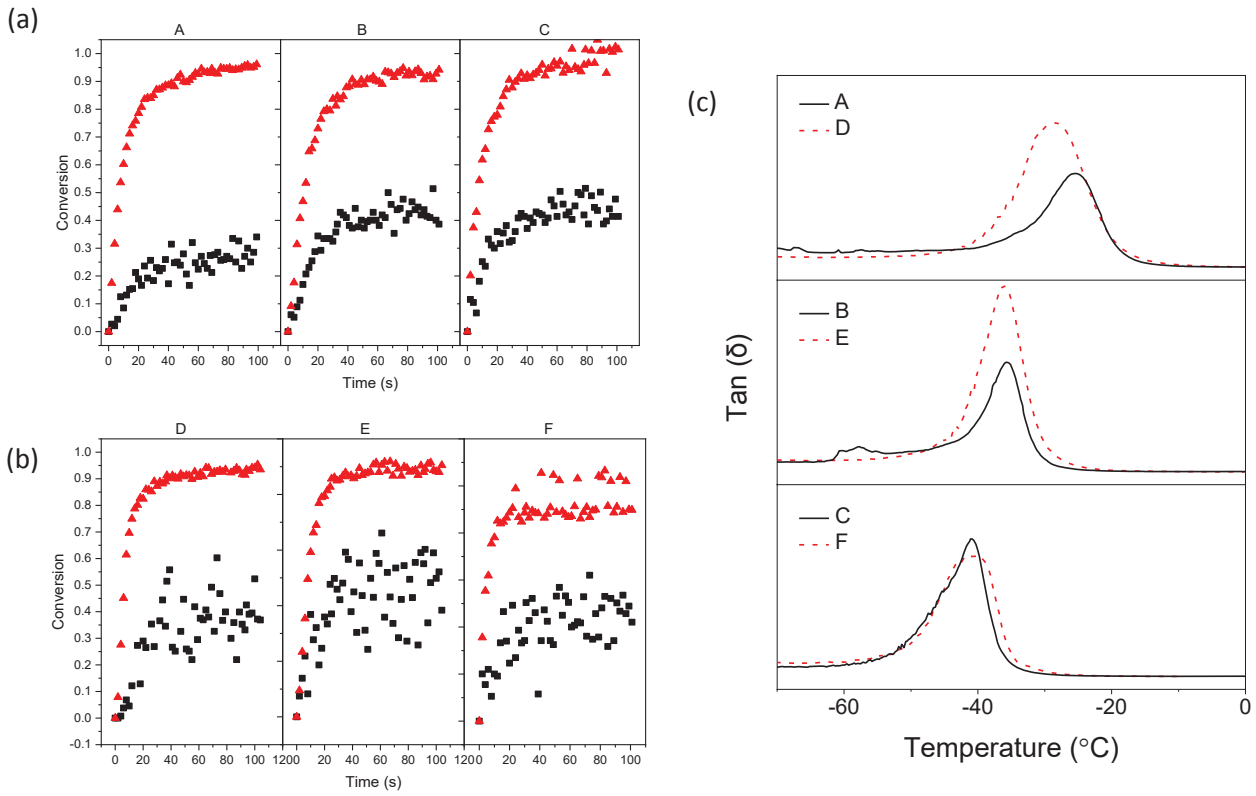

Figure 2: Evolution of thiol (black squares) and acrylate (red triangles) functional group conversion with time measured by FTIR for (a) samples A-C, and (b) samples D-F (see Table 1), and (c) DMA of *net*-poly(PEG$_x$DA-*co*-TMPTMP) samples A to F, for x=3 (top), x =10 (middle), and x =13 (bottom). Continuous lines correspond to samples A-C prepared via TMPTMP/PEG diacrylate copolymerization. Dashed lines correspond to the analogous samples D-F synthesized via the STMRT strategy using the polymeric tetrathiols **4**-**6** and PEG diacrylates **1**-**3**.

Stepwise synthesis of trithiol/acrylate binary model networks via Sequential thiol-Michael - radical thiol-ene (STMRT)

The thiol-Michael reaction leads to selective, single addition of thiols to acrylates. In this way, we reacted the TMPTMP and PEGDA and we obtained the polymeric tetrathiols **4**-**6**, as depicted in Scheme 1. Through thiol-ene copolymerization of tetrathiols **4-6** with PEGDA of the same M_n (i.e. the STMRT method) the model network systems **D-F** were obtained. As the precursors for **D**-**F** are the same as **A-C**, the polymers are inherently the same with respect to monomeric components (e.g. *net*-poly(PEG$_x$DA-*co*-TMPTMP) with the exception that the sequential polymerization thiol-Michael step was employed. The properties of these networks are thus directly compared with **A-C**.

It can be observed by photo-FTIR of the STMRT systems **D**-**F,** that the acrylate groups are consumed more rapidly than the thiols (see Figure 2 (b)). The final conversion of acrylate (and thiol) groups for samples **D, E** and **F** are estimated as 93% (39%), 89% (46%), and 94% (45%) respectively (see Table 1). This difference in rate of consumption was also observed for the analogous samples **A**-**C** discussed above. Indeed, the acrylate and thiol conversions for the two types of systems are similar (see Figures 2 (a) and (b)). Again, the theoretical heat of reaction per thiol for sample **D**-**F**, calculated using the photo-FTIR conversion data, correlated well with the photo-DSC data (see Table 1 and Figure S16).

The systems derived from the two synthetic methods differ in the heat released during photopolymerization (network formation). The thiol-Michael "pre-reaction" reduces the enthalpy of reaction per gram as observed in photo-DSC for the STMRT systems **D-F** (see Table 1). Note, the enthalpy per mole is similar in both systems (see Table 1). The differing synthetic approaches lead to differences in material properties. For example, the T_g shifted. This appears to be influenced by chain length and is most noticeable when comparing DMA profiles for the systems derived from the shortest PEG segments **A** and **D** (see Table 1 and see Figure 2(c)). The tan(δ) peaks are broader for the STMRT samples **D-F**, as evidenced by the increase in the full width at half maximum (FWHM) (i.e. 8.7 °C, 6.3 °C, and 7.7 °C for A-C respectively, and 10.9 °C, 7.2 °C, and 9.9 °C for D-F respectively).

Networks through trithiol/diacrylate/divinyl ether terpolymerization

Vinyl ethers and acrylates display different reactivity and reaction kinetics with respect to the radical thiol-ene reaction. To further probe the use of STMRT strategy, a combination of these two different alkene functionalities in a ratio of acrylate:vinyl ether 1:2 was investigated.

Thiyl radical addition (the key addition step in radical thiol-ene) to electron-rich vinyl ethers is faster than to electron-poor acrylates. In contrast, radical homopolymerization of vinyl ethers is orders of magnitude slower than other possible reactions in the system. Indeed, some theoretical and kinetic studies on these ternary systems neglect vinyl ether homopolymerization in their models for this reason.[4, 21] However, in copolymerization systems, there is evidence for cross-propagation, in which a vinyl ether derived radical reacts with acrylate, driven by the higher stability of acrylate-derived radicals and polar effects.[9] Overall, reactions with vinyl ethers are more selective towards radical thiol-ene addition than are acrylates as there is little homopolymerization.

Three network systems analogous to **A-C** were prepared, where PEGDA was replaced by TEGDVE:PEGDA 2:1 to yield samples **G-I**. To study ternary systems two plots from the photo-FTIR can be prepared. In Figure 3 (a) the conversion of thiol and total alkene (i.e. vinyl ether + acrylate) is plotted (for detailed comparison of vinyl ether and acrylate conversion see Figure S15 in the supporting information). The final conversion of total alkene (and thiol) groups for samples **G, H** and **I** are estimated as 97% (69%), 93% (93%), and 92% (92%), respectively (see Table 1; where individual conversions of acrylate and vinyl ether alkene groups are given). In these ternary systems, the trend is similar to that seen with binary acrylate/thiol samples, in which alkene homopolymerization is lower for increasing PEG chain length. There is also a higher (heat of reaction) enthalpy per mole with increased PEG chain length – indicating an increasing preference for the thiol-ene reaction pathway over radical polymerization of the alkene. Note, again the theoretical heat of reaction per thiol for sample **G**-**I**, calculated using the photo-FTIR conversion data, correlates well with the photo-DSC data (see Table 1 and Figure S16). We hypothesise that increasing the PEG chain length delays the gel point, leading to higher conversions. This is also noticeable in a slight increase in T_g of sample **I** compared to **C**, but mechanical properties of the final networks **A-C** and **G-I** are very similar in terms of T_g, FWHM, and E' (see Figure 3 (c), solid black lines).

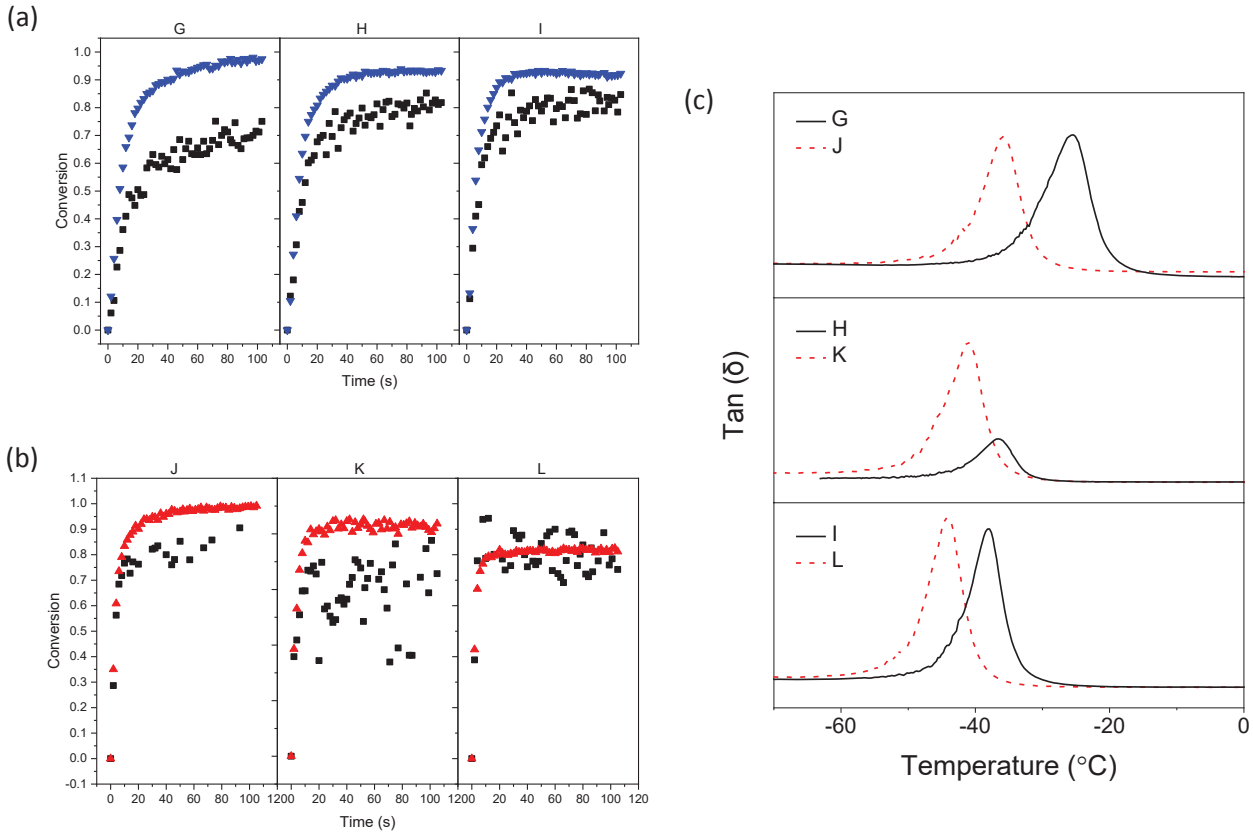

Figure 3: Evolution of functional group conversion with time measured by FTIR for (a) samples **G**-**I** (thiols, black squares; alkenes (acrylates + ether vinyls), blue triangles) and (b) samples **J**-**L** (thiols, black squares; ether vinyls, red triangles) (see Table 1) and (c) DMA of *net*-poly(PEG$_x$DA-*co*-TEGDVE-*co*-TMPTMP) samples G to L, for x=3 (top), x =10 (middle), and x =13 (bottom). Continuous black lines correspond to samples **G**-**I** prepared via TMPTMP/PEG$_x$DA/TEGDVE terpolymerization. Dashed red lines correspond to the analogous samples **J**-**L** synthesized via the STMRT strategy using the polymeric tetrathiols **4**-**6** & TEGDVE.

Stepwise synthesis of ternary trithiol/diacrylate/divinyl ether model networks via sequential thiol-Michael - radical thiol-ene (STMRT)

Similar to the STMRT copolymer samples **D-F**, for the synthesis of the STMRT terpolymers PEGDA was first reacted with two equivalents of TMPTMP by thiol Michael addition to yield macromolecular tetrathiols **4-6**. This "pre-reaction" has an additional effect in these ternary systems of preventing kinetic competition between acrylate and vinyl ether alkenes. The samples obtained, **J-L** (see Table 1), are studied by photo-FTIR, DMA, and photo-DSC. These samples can be directly compared to the samples **G**-**I** discussed in the previous section as their constituent components are the same, and thus enable the direct examination of the effect of the STMRT process.

The trend in the conversion of the thiol groups during the preparation of samples **J-L** (see Figure 3 (b)) differs from that observed in **G-I** (see Figure 3 (a)), with the STRMT samples **J**-**L** displaying almost constant thiol conversion across all the systems. This is in contrast to the analogous ternary **G**-**I** samples, where the thiol conversion increased with PEG chain length (Figure 3 (a) and Table 1). The final conversion of alkene (and thiol) groups for samples **J, K** and **L** are estimated as 98% (86%), 83% (59%), and 82% (78%) respectively (see Table 1). This is due to the absence of the competing alkene homopolymerization in the absence of free acrylate groups, which, as stated previously, are prone to undergo this side reaction. The theoretical heat of reaction per thiol for sample **J-L**, calculated using the photo-FTIR conversion data, corresponded well with the photo-DSC data (see Table 1 and Figure S16). Despite thiol conversion being almost constant across the STMRT products **J**-**L**, differences in T_g are observed across the samples; the T_g, as expected, decreases with increasing PEG chain length (see Figure 3 (c) and Table 1). This observation is in contrast with binary TMPTMP/PEGDA systems, in which STMRT didn't have a drastic impact on T_g.

It is important to note that in STMRT samples **J-L** the difference between thiol and alkene conversion is small. This shows these networks are mainly formed by radical thiol-ene addition and results in a more homogeneous blend of PEG and triethyleneglycol segments in the network structure. A network formed purely by thiol-ene addition displays lower crosslink density than one formed (even partially) by alkene homopolymerization; this is because alkenes only form one bond through thiol-ene addition (functionality of one) but they form two by homopolymerization (functionality of two). This results (see Figure 3(c)) in a lower T_g and tan(δ) peaks in DMA that are as sharp as those observed in simple binary thiol-ene systems like **A-C**.

These results from these ternary systems clearly show that a distinct difference in the thermomechanical properties is achievable through careful manipulation of network precursors.

Conclusions

Analysis of several photopolymerised thiol-ene networks comprising acrylate and/or vinyl ether systems was conducted by DMA, photo-DSC, and phot-FTIR. The stepwise preparation of the networks by sequential thiol-Michael - radical thiol-ene (STMRT) strategy was compared to the more traditional 'one pot' approach, by examining the effects of altering the reaction components and the PEG chain length.

We find that increasing the PEG chain length in binary PEGDA + TMPTMP (**A-C**) networks results in higher extent of thiol-ene reaction, and that the amount of acrylate homopolymerization heavily influences the material properties. Preparation of polymeric PEG-$(SH)_4$ tetrathiols **4**-**6** before network formation (**D-F**) (i.e. STRMT) results in increased thiol-ene linkages within the networks. These systems displaye an increase in FWHM of tan(δ) peaks, implying the formation of networks comprise multimodally distributed polymer chain lengths.

The ternary TMPTMP + PEGDA + TEGDVE systems (**G-I**) showed a similar trend for increased extent of thiol-ene addition as PEG chain length increases, as well as higher conversion of thiol than in binary thiol-acrylate systems due to the increased selectivity of vinyl ether alkene groups towards thiols compared to acrylates-based alkenes. The T_g again is seen to decrease with increasing PEG chain length, which indicates that crosslinks per unit of volume decreases with increasing wt% of PEG in the network.

The preparation of analogous ternary networks via the STMRT approach using the polymeric tetrathiols **4**-**6** and TEGDVE delivered homogeneous networks of TEGDVE and PEGDA. These materials all displayed reduced T_g for all three PEG lengths and much narrower tan(δ) FWHM than the corresponding ternary systems **G-I** prepared through standard methods.

We have shown that the STMRT strategy has a small effect on crosslink density and the resulting material properties of networks that display significant alkene homopolymerization during their preparation (i.e. acrylates), irrespective of whether they are binary or ternary monomer systems. Conversely, the stepwise STMRT strategy paves the way to the synthesis of thiol-ene photocrosslinked networks with a much wider variety of macromonomers of designed functionality, while preventing competition between thiol-ene addition and alkene homopolymerization; this is particularly pertinent for acrylic-based (and related) systems. Networks prepared in this stepwise manner are formed solely by thiol-ene addition and their properties can therefore be tailored to meet any desired crosslink density. The control over crosslink density and functionality is crucial for controlling mechanical properties of network materials.

Conflicts of interest

There are no conflicts to declare

Acknowledgements

The Authors gratefully acknowledge the Polymer Characterization Research Technology Platform, University of Warwick for access to instrumentation for polymer characterization (DMA and PhotoDSC) and the Faculty of Science and Engineering, University of Wolverhampton for access to NMR. The authors would also like to thank Miss Beth Dickens for conducting some initial pilot experiments prior to the work in this publication.

Notes

§ Quantitative analysis may be conducted using proton-decoupled ^{13}C NMR provided resonances of the same type are compared (in this case methylenes, CH_2); see Otte et al.[28] for further information.

§§ The two expected ^{13}C NMR signals arising from the two different types of ester-adjacent methylene (CH_2) groups are coincident at 63.8 ppm for each of the PEG-tetrathiols (**4**-**6**). This does not hinder the integration analysis discussed.

References

1. A. B. Lowe, *Polymer Chemistry*, 2014, **5**, 4820-4870.
2. N. B. Cramer and C. N. Bowman, in *Thiol-X Chemistries in Polymer and Materials Science*, The Royal Society of Chemistry, 2013, DOI: 10.1039/9781849736961-00001, ch. 1, pp. 1-27.
3. I. Mita, R. F. T. Stepto and U. W. Suter, *Pure and Applied Chemistry*, 1994, **66**, 2483-2486.
4. S. K. Reddy, O. Okay and C. N. Bowman, *Macromolecules*, 2006, **39**, 8832-8843.
5. O. Okay, S. K. Reddy and C. N. Bowman, *Macromolecules*, 2005, **38**, 4501-4511.
6. O. Okay and C. N. Bowman, *Macromolecular Theory and Simulations*, 2005, **14**, 267-277.
7. A. F. Jacobine, D. M. Glaser, P. J. Grabek, D. Mancini, M. Masterson, S. T. Nakos, M. A. Rakas and J. G. Woods, *Journal of Applied Polymer Science*, 1992, **45**, 471-485.
8. J. G. Woods, *Radiation-curable adhesives*, 1992.
9. C. E. Hoyle, T. Y. Lee and T. Roper, *Journal of Polymer Science Part A: Polymer Chemistry*, 2004, **42**, 5301-5338.
10. A. S. Quick, J. Fischer, B. Richter, T. Pauloehrl, V. Trouillet, M. Wegener and C. Barner-Kowollik, *Macromolecular Rapid Communications*, 2013, **34**, 335-340.
11. E. Blasco, M. Wegener and C. Barner-Kowollik, *Adv. Mater.*, 2017, **29**, 1604005.
12. L. M. Campos, I. Meinel, R. G. Guino, M. Schierhorn, N. Gupta, G. D. Stucky and C. J. Hawker, *Advanced Materials*, 2008, **20**, 3728-3733.
13. D. Foix, X. Fernández-Francos, X. Ramis, A. Serra and M. Sangermano, *Reactive and Functional Polymers*, 2011, **71**, 417-424.
14. Y. B. Kim, H. K. Kim, H. C. Choi and J. W. Hong, *Journal of Applied Polymer Science*, 2005, **95**, 342-350.
15. H. Wei, Q. Li, M. Ojelade, S. Madbouly, J. U. Otaigbe and C. E. Hoyle, *Macromolecules*, 2007, **40**, 8788-8793.
16. A. F. Senyurt, H. Wei, C. E. Hoyle, S. G. Piland and T. E. Gould, *Macromolecules*, 2007, **40**, 4901-4909.
17. Q. Li, H. Zhou and C. E. Hoyle, *Polymer*, 2009, **50**, 2237-2245.
18. A. F. Senyurt, H. Wei, B. Phillips, M. Cole, S. Nazarenko, C. E. Hoyle, S. G. Piland and T. E. Gould, *Macromolecules*, 2006, **39**, 6315-6317.
19. 1995.
20. B. D. Fairbanks, T. F. Scott, C. J. Kloxin, K. S. Anseth and C. N. Bowman, *Macromolecules*, 2009, **42**, 211-217.
21. N. B. Cramer and C. N. Bowman, *Journal of Polymer Science Part A: Polymer Chemistry*, 2001, **39**, 3311-3319.
22. H. E. Gottlieb, V. Kotlyar and A. Nudelman, *J. Org. Chem.*, 1997, **62**, 7512-7515.
23. W. D. Cook, T. L. Schiller, F. Chen, C. Moorhoff, S. H. Thang, C. N. Bowman and T. F. Scott, *Macromolecules*, 2012, **45**, 9734-9741.
24. D. Nwabunma, K. J. Kim, Y. Lin, L. C. Chien and T. Kyu, *Macromolecules*, 1998, **31**, 6806-6812.
25. T. Clark, L. Kwisnek, C. E. Hoyle and S. Nazarenko, *Journal of Polymer Science Part A: Polymer Chemistry*, 2009, **47**, 14-24.
26. T. M. Roper, T. Kwee, T. Y. Lee, C. A. Guymon and C. E. Hoyle, *Polymer*, 2004, **45**, 2921-2929.
27. T. M. Roper, C. E. Hoyle and D. H. Magers, in *Photochemistry and UV curing: new trends*, ed. J. P. Fouassier, Research Signpost, 2006, ch. 22, pp. 253-264.
28. D. A. L. Otte, D. E. Borchmann, C. Lin, M. Weck and K. A. Woerpel, *Organic Letters*, 2014, **16**, 1566-1569.
29. A. E. Rydholm, C. N. Bowman and K. S. Anseth, *Biomaterials*, 2005, **26**, 4495-4506.
30. M. Furutani, T. Ide, S. Kinoshita, R. Horiguchi, I. Mori, K. Sakai and K. Arimitsu, *Polymer International*, 2019, **68**, 79-82.
31. C. Chen, A. M. Eissa, T. L. Schiller and N. R. Cameron, *Polymer*, 2017, **126**, 395-401.
32. D. W. Johnson, C. R. Langford, M. P. Didsbury, B. Lipp, S. A. Przyborski and N. R. Cameron, *Polymer Chemistry*, 2015, **6**, 7256-7263.